Class E DC/DC Converters with an Inductive Impedance Inverter

MARIAN K. KAZIMIERCZUK AND XUNG T. BUI

Abstract—**The analysis, design equations, and experimental verification are presented for a Class E dc/dc switching-mode high-efficiency resonant dc/dc power converter with a transformer center-tapped rectifier. The analysis is performed at a constant current through the dc-feed choke and using the high-Q_l assumption ($Q_l \geq 5$). The converter may operate under safe conditions for load resistances ranging from a full load to an open circuit. This feature has been accomplished by using an inductive impedance inverter. The results of the analysis are then generalized for the entire family of Class E dc/dc converters. Experimental results show good agreement with the theoretical predictions. The measured total efficiency was 89 percent at 1 MHz with 15 W output power. A narrow-band FM regulation ($\Delta f/f$ = 12 percent) of the dc output voltage was achieved as the load was varied from a minimum resistance (full load) to an open circuit.**

I. Introduction

CLASS E switching-mode tuned power inverters [1]–[20] can operate efficiently in the megahertz frequency range. They are particularly suited for high-frequency operation because 1) the turn-on switching loss is zero, yielding high efficiency and 2) the transistor output capacitance is absorbed into the external shunt capacitance. Class E resonant dc/dc converters [21]–[32] were derived from Class E inverters by adding rectifiers at the inverter output. The purpose of this paper is to 1) present an analysis and design rules for a Class E dc/dc converter with a transformer center-tapped rectifier and an inductive impedance inverter given in [25], [26], and 2) extend the results for other topologies of Class E dc/dc converters analyzed in [31].

Fig. 1(a) shows a circuit of the Class E dc/dc converter. It consists of a Class E inverter and a transformer center-tapped full-wave rectifier. The Class E inverter is composed of a power MOSFET, an antiparallel diode $D1$, a radio frequency (RF) choke L_1, and a resonant circuit C_1-C_2-L_2-L_3. The power MOSFET and the antiparallel diode $D1$ form a bidirectional switch S which turns on and off at the switching frequency $f = \omega/2\pi$. The inductor L_3 has two tasks: 1) it acts as a matching network and 2) as an inductive impedance inverter [27]. The shape of the current i depends on the loaded quality factor Q_l and the ON switch duty cycle D [17]. The current i is approximately sinusoidal for $Q_l \geq 5$ and $D \geq 0.5$. Therefore, the output power of the inverter is approximately composed of only the fundamental component. The analysis of the inverter for optimum operation is given in [17] and for nonoptimum operation in [18] at any Q_l and D. There are two modes of rectifier operation, the continuous mode and the discontinuous mode. Figs. 2 and 3 show the current and voltage waveforms for these modes. This paper is focused upon interfacing the inverter and the rectifier.

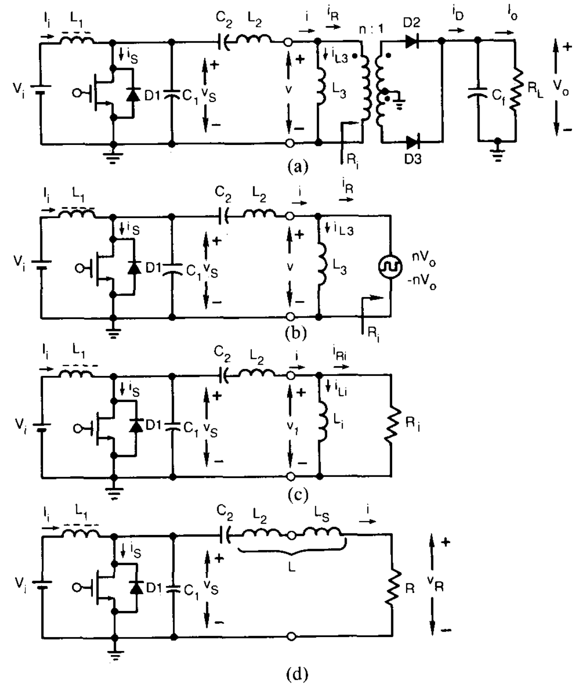

Fig. 1. Class E dc/dc converter. (a) Circuit. (b) Equivalent circuit. (c) Circuit of Class E inverter with matching network. (d) Basic circuit of Class E inverter.

The converter analysis is based on the following assumptions.

1) The RF choke inductance L_1 is large enough so that the dc ripple current in the input current I_i is negligible.

2) The loaded quality factor Q_l of the resonant circuit is high ($Q_l \geq 5$) so that the current i is a sine wave and, therefore, the inverter output power is composed of the fundamental component only.

3) The converter components are ideal.

Manuscript received February 4, 1988; revised July 20, 1988. This work was supported under the Ohio State Research Challenge Grant, No. 660-763.

M. K. Kazimierczuk is with the Department of Electrical Systems Engineering, Wright State University, Dayton, OH 45435.

X. T. Bui is with SofTech Inc., 3100 Presidential Drive, Fairborn, OH 45324.

IEEE Log Number 8824131.

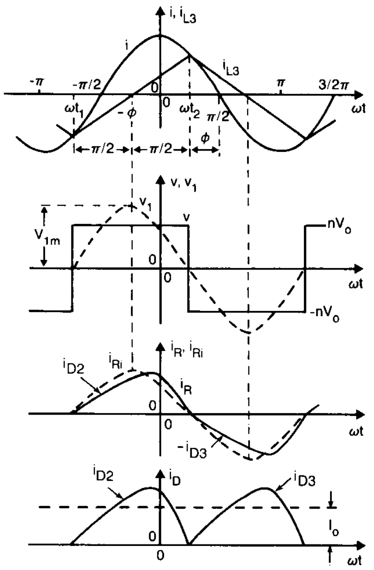

Fig. 2. Current and voltage waveforms in Class E dc/dc converter for continuous mode of operation.

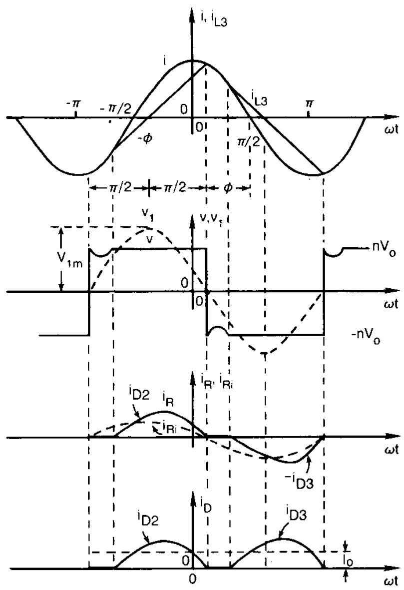

Fig. 3. Current and voltage waveforms in Class E dc/dc converter for discontinuous mode of operation.

II. Analysis

The analysis of the converter for the continuous mode of operation is presented below. Under the high-Q_1 assumption ($Q_1 \geq 5$), the current i in the L_2-C_2 branch is approximately a cosine wave [17] given by

$$i = I_m \cos \omega t \tag{1}$$

where I_m is the amplitude of i. Neglecting the voltage drop across the rectifier diodes $D2$ and $D3$, the voltage v at the input of the transformer is a square wave with the magnitudes nV_o and $-nV_o$, i.e.,

$$v = \begin{cases} nV_o, & \text{for } -\dfrac{\pi}{2} - \phi < \omega t \leq \dfrac{\pi}{2} - \phi \\ -nV_o, & \text{for } \dfrac{\pi}{2} - \phi < \omega t \leq \dfrac{3\pi}{2} - \phi. \end{cases} \tag{2}$$

The transformer/rectifier circuit can be replaced with a square-wave voltage source as shown in Fig. 1(b). The fundamental component of the voltage v is given by

$$v_1 = V_{1m} \cos(\omega t + \phi) \tag{3}$$

where

$$V_{1m} = \frac{4nV_o}{\pi}. \tag{4}$$

is the amplitude of v_1 and ϕ is the initial phase of v_1. The rms value of v_1 is

$$V_1 = \frac{V_{1m}}{\sqrt{2}} = \frac{4nV_o}{\pi\sqrt{2}}. \tag{5}$$

The dc-to-ac voltage transfer function of the rectifier is

$$M_R = \frac{V_o}{V_1} = \frac{\pi\sqrt{2}}{4n} = \frac{\pi}{2\sqrt{2}n} \simeq \frac{1.11}{n}. \tag{6}$$

Since the voltage v across the inductance L_3 is a square wave, the current i_{L3} is a symmetrical triangle wave. The slope of i_{L3} is $i_{L3}(\omega t_2)/(\pi/2)$, where $\omega t_2 = \pi/2 - \phi$. From (1), $i_{L3}(\omega t_2) = i(\omega t_2) = I_m \cos(\pi/2 - \phi) = I_m \sin \phi$. Thus the current i_{L3} is

$$i_{L3} = \frac{2I_m \sin \phi}{\pi}(\omega t + \phi). \tag{7}$$

From (1) and (7), the input current of the transformer is

$$i_R = i - i_{L3} = I_m \cos \omega t - \frac{2I_m \sin \phi}{\pi}(\omega t + \phi). \tag{8}$$

Thus, the current i_D at the input of the C_f-R_L circuit is

$$\begin{aligned} i_D &= i_{D2} + i_{D3} = n|i_R| \\ &= \left| nI_m \cos \omega t - \frac{2nI_m \sin \phi}{\pi}(\omega t + \phi) \right|. \end{aligned} \tag{9}$$

Hence, the dc output current is

$$I_o = \frac{1}{\pi}\int_{-\pi/2-\phi}^{\pi/2-\phi} i_D d(\omega t) = \frac{2nI_m \cos \phi}{\pi}, \tag{10}$$

from which (7) becomes

$$i_{L3} = \frac{I_o \tan \phi}{n}(\omega t + \phi). \tag{11}$$

Substituting (2) and (11) into $v = X_{L3} di_{L3}/d(\omega t)$, one obtains

$$nV_o = X_{L3}\frac{di_{L3}}{d(\omega t)} = \frac{I_o X_{L3} \tan \phi}{n} \tag{12}$$

where $X_{L3} = \omega L_3$. Since $R_L = V_o/I_o$, (12) reduces to

$$\tan\phi = \frac{n^2 R_L}{X_{L3}}. \quad (13)$$

The voltage v at the input of the inductance L_3 is a square wave. It contains odd harmonics. However, since the current i contains only the fundamental component, the power at the input of L_3 also contains only the fundamental component P_1. This power is converted into the dc output power P_o. From (4) and (10),

$$P_1 = \frac{I_m V_{1m}}{2}\cos\phi = I_o V_o = P_o. \quad (14)$$

The current i_{L3} is an odd periodic function with respect to $\omega t = -\phi$. It contains only odd sine terms in its Fourier series representation. For example, the fundamental component of i_{L3} is $i_{L31m} = I_{L31m}\sin(\omega t + \phi)$, where $I_{L31m} = 8I_m \sin\phi/\pi^2$. The current i_R exhibits half-wave symmetry and, therefore, it contains odd cosine and odd sine terms. Since the voltage v contains only odd cosine terms, the input power of the transformer also contains only odd components. All these components are converted into the dc output power P_o. The analysis based on an infinite number of components is difficult to perform. Therefore, an easier approach is presented below.

Fig. 1(c) shows an L_i-R_i model of the input impedance of the circuit composed of the inductor L_3, transformer, and rectifier. This model is determined at the fundamental frequency f. The L_i-R_i model is created in such a way that the power P_1 given by (14) is delivered to R_i at the fundamental frequency f exclusively. The currents through R_i and $X_i = \omega L_i$ are

$$i_{Ri} = I_{Rim}\cos(\omega t + \phi) \quad (15)$$

$$i_{Li} = I_{Lim}\sin(\omega t + \phi). \quad (16)$$

Fig. 4 depicts the phasor diagram of the fundamental components I_{Rim}, I_{Lim}, I_m, and V_{1m}, which leads to

$$I_{Rim} = I_m\cos\phi \quad (17)$$

$$I_{Lim} = I_m\sin\phi. \quad (18)$$

Note that I_{L31m} is less than I_{Lim} by a factor of $8/\pi^2$. Substitution of (17) into (10) gives

$$I_o = \frac{2nI_{Rim}}{\pi}. \quad (19)$$

This is a well-known expression for the dc output current in a full-wave rectifier without filter capacitor. Using (4), (19), and $R_L = V_o/I_o$, one obtains

$$R_i = \frac{V_{1m}}{I_{Rim}} = \frac{8n^2}{\pi^2}R_L \simeq 0.81n^2R_L. \quad (20)$$

The same expressions can be derived as follows. The total input power of the transformer is $P_{Ri} = V_{1m}^2/(2R_i) = 8n^2V_o^2/(\pi^2R_i)$ and the dc output power is $P_o = V_o^2/R_L$. Since $P_o = P_{Ri}$, one obtains (20). From Fig. 4, (20), I_{Rim}

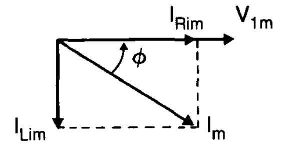

Fig. 4. Phasor diagram of fundamental components.

$= V_{1m}/R_i$, and $I_{Lim} = V_{1m}/X_i$,

$$\tan\phi = \frac{I_{Lim}}{I_{Rim}} = \frac{R_i}{X_i} = \frac{8n^2R_L}{\pi^2X_i}. \quad (21)$$

Comparing (13) and (21) results in

$$X_i = \frac{8}{\pi^2}X_{L3}. \quad (22)$$

Thus, the relationships among R_i, X_i, R_L, and X_{L3} are given by (20), (21), and (22). The circuit of Fig. 1(c) is a Class E inverter with a matching load network. At the fundamental frequency f, the L_i-R_i parallel combination can be converted into an L_S-R series combination resulting in the basic topology of the Class E inverter, shown in Fig. 1(d).

If the dc output voltage is low (e.g., $V_o = 5$ V), the voltage drop V_F across the conducting rectifier diodes can be taken into account [31]. In this case, one obtains $v = \pm n(V_o + V_F)$, $V_{1m} = 4nV_o(1 + V_F/V_o)/\pi$, $M_R = \pi/[2\sqrt{2}n(1 + V_F/V_o)] \simeq 1.11/[n(1 + V_F/V_o)]$, $R_i = 8n^2R_L(1 + V_F/V_o)/\pi^2 \simeq 0.81n^2R_L(1 + V_F/V_o)$, and the rectifier efficiency $\eta_R = 1/(1 + V_F/V_o)$.

The boundary between the continuous and discontinuous modes of operation occurs when $di_{L3}/d(\omega t) = di/d(\omega t)$ at $\omega t_1 = -\pi/2 - \phi_{cr}$, where ϕ_{cr} is the critical value of ϕ at the boundary. Hence, from (1) and (7),

$$\tan\phi_{cr} = \frac{\pi}{2}, \quad (23)$$

from which $\phi_{cr} = 57.52°$. For $\phi < \phi_{cr}$, the rectifier acts in the continuous mode of operation, shown in Fig. 2. From (20), (21), and (22), this mode occurs for

$$R_i < \frac{\pi}{2}X_i = \frac{4}{\pi}X_{L3}, \quad (24)$$

or equivalently,

$$R_L < \frac{\pi}{2n^2}X_{L3}. \quad (25)$$

Substitution of (10) into (9) results in i_D in terms of I_o:

$$i_D = I_o\left|\frac{\pi\cos\omega t}{2\cos\phi} - (\tan\phi)(\omega t + \phi)\right|. \quad (26)$$

The peak forward current I_{DM} of the rectifier diodes i_{D2} and i_{D3} is determined by $di_D/d(\omega t) = 0$. Hence, from (26), the maximum value of i_D occurs at

$$\omega t_{max} = -\arcsin\left(\frac{2\sin\phi}{\pi}\right). \quad (27)$$

Substitution of this into (26) gives I_{DM}, e.g., $I_{DM}/I_o = \pi/2 = 1.57$ at $\phi = 0°$, $I_{DM}/I_o = 1.665$ at $\phi = 45°$, and $I_{DM}/I_o = 1.774$ at $\phi = 57°$. The peak reverse voltages of the rectifier diodes are

$$V_{D2MR} = V_{D3MR} = -2V_o. \tag{28}$$

For $\phi > \phi_{cr}$, the rectifier operates in the discontinuous mode, illustrated in Fig. 3. When $i_R = i - i_{L3}$ is positive, diode $D3$ conducts. When $i_R = i - i_{L3}$ is negative, diode $D2$ conducts. However, there are time intervals when both diodes are OFF. Then (neglecting the parasitic capacitances of the two diodes), the C_1-C_2-L_2-L_3 resonant circuit is disconnected from the C_f-R_L circuit and resonates like an unloaded tank. Consequently, the voltage v is no longer a square wave and the current i_{L3} is no longer a triangle wave. The waveforms in the experimental circuit will be shown in Section VII.

III. Impedance Inverter

The optimum operation of the basic Class E inverter of Fig. 1(d) occurs at the optimum load resistance $R = R_{opt}$ [1]–[19]. The lossless operation of the inverter can be obtained for $0 \le R \le R_{max} = R_{opt}$. In contrast, the converter load resistance R_L is usually in the range $R_{L\min} \le R_L < \infty$. According to (17), the rectifier input resistance R_i is proportional to R_L. Hence, the range of R_i is $R_{i\min} \le R_i < \infty$. Clearly, an impedance inverter is required between the Class E inverter and the rectifier to remove the impedance incompatibility.

The circuit of Fig. 1(c) is a Class E inverter with a C_1-C_2-L_2-L_i matching load network in which an impedance inversion can be achieved [27]. Fig. 1(d) shows its equivalent circuit obtained by using the equivalent two-terminal networks method. The relationships among the component values at the operating frequency f are as follows [27]:

$$q_B = \frac{R_i}{X_i} = \tan\phi \tag{29}$$

$$R = \frac{R_i}{1 + q_B^2} = \frac{R_i}{1 + \left(\frac{R_i}{X_i}\right)^2} \tag{30}$$

$$X_{LS} = \frac{X_i}{1 + \frac{1}{q_B^2}} = \frac{X_i}{1 + \left(\frac{X_i}{R_i}\right)^2} \tag{31}$$

$$X_L = \omega L = X_{L2} + X_{LS}. \tag{32}$$

Expressions (30) and (31) are plotted in Fig. 5.

From (30), $dR/dR_i = 0$ at $R_i = X_i$, i.e., at $q_B = 1$. Substitution of this into (30) yields the maximum value of R:

$$R_{max} = \frac{X_i}{2}.$$

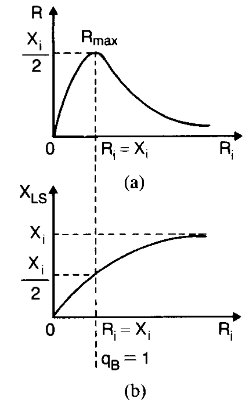

Fig. 5. Relationships among R, R_i, X_i, and X_{LS}. (a) R as a function of R_i. (b) X_{LS} as a function of R_i.

For $R_i = X_i$, (31) becomes

$$X_{LS} = \frac{X_i}{2}.$$

For $q_B^2 >> 1$, i.e., $R_i >> X_i$,

$$R \simeq \frac{X_i^2}{R_i}, \qquad X_{LS} \simeq X_i.$$

For $q_B = 0$, i.e., for $R_i = 0$, $R = 0$, and $X_{LS} = 0$.

The conclusions are as follows.

1) $R \le X_i/2 = 4X_{L3}/\pi^2$ at any value of R_i, i.e., at any value of R_L.

2) For $q_B \ge 1$, R decreases as R_i increases, i.e., as R_L increases. Thus the circuit acts like an *impedance inverter*.

3) For $q_B^2 >> 1$, R is *inversely proportional* to R_i and $X_{LS} \simeq X_i = 8X_{L3}/\pi^2$ is approximately independent of R_i, i.e., R_L.

4) If $R_{opt} = R_{max} = X_i/2$, the range of R is $0 \le R \le R_{opt}$ for $0 \le R_i \le \infty$, i.e., for $0 \le R_L \le \infty$. Thus, the Class E inverter acts under lossless (zero-voltage-switching) conditions at any R_i, i.e., at any R_L, including a short circuit ($R_L = 0$) and an open circuit ($R_L = \infty$).

5) If $R_{opt} < R_{max} = X_i/2$, the lossless converter operation can be obtained for $0 \le R_i \le R_{i\max}$ and $R_{i\min} \le R_i \le \infty$. Thus, there is a gap in R_i (and therefore also in R_L) in which the lossless operation cannot be achieved. However, R is less sensitive to R_i for $R_{i\min} \le R_i \le \infty$ and thereby a narrower bandwidth of the switching frequency f is required to control V_o.

Note that for $R_L = \infty$, $R_i = \infty$ and therefore the load network consists of C_1, L_2, and L_3. For $R_L = 0$, $R_i = 0$ and thereby the load network consists of C_1, L_2 and C_2. In both cases, the series-resonant circuit is closed. In the basic topology of the Class E converter [31], the series-resonant circuit is open at $R_L = \infty$.

IV. DC Voltage Transfer Function

First, the ac-to-dc voltage transfer function will be determined for the Class E inverter of Fig. 1(d). The dc input power of the inverter is $P_i = I_i V_i = V_i^2/R_{dc}$, where $R_{dc} = V_i/I_i$ is the dc input resistance of the inverter. The ac output power of the inverter is $P_{oA} = V_R^2/R$, where V_R is the rms value of the inverter output voltage v_R which may be either sinusoidal or nonsinusoidal depending on Q_1 and D [17]. Hence, $V_R = \sqrt{P_{oA}R}$. Assuming that the inverter efficiency is $\eta_A = 100$ percent, $P_{oA} = P_i$. Thus, the ac-to-dc voltage transfer function of the Class E inverter is

$$M_A = \frac{V_R}{V_i} = \sqrt{\frac{P_{oA}R}{V_i^2}} = \sqrt{\frac{P_{oA}R}{P_i R_{dc}}} = \sqrt{\frac{R}{R_{dc}}}. \quad (33)$$

The values of $M_A^2 = P_{oA}R/V_i^2$ are given in [17] for optijmum operation at any values of Q_1 and D. Using these results, the values of M_A were calculated and are given in Table I. As seen, M_A increases with D and Q_1. A close examination reveals that the values of M_A are in the range of $0 < M_A < \sqrt{2}$ for optimum operation. For $Q_1 \geq 5$, the voltage v_R is nearly a sine wave [17].

The efficiency of the actual inverter $\eta_A = P_{oA}/P_i$ is less than 100 percent. Hence, from (33),

$$M_A = \sqrt{\frac{\eta_A R}{R_{dc}}}. \quad (34)$$

For example, at $\eta_A = 95$ percent (which is a typical value of η_A for $f \leq 3$ MHz and $V_i \geq 12$ V), $\sqrt{\eta_A} = 0.975$. Thus, M_A of the actual inverter will be lower than that of the ideal inverter by 2.5 percent.

The conduction power loss in a MOSFET is $P_{CDS} = 2.37 r_{DS} I_i^2$ at $D = 0.5$ and $Q \geq 5$ for optimum operation, where r_{DS} is the transistor on-resistance. The efficiency of the resonant circuit is $\eta_o = 1 - Q_1/Q_o$, where Q_o is the unloaded quality factor of the resonant circuit associated with a series equivalent ac resistance r_L of L and a series ac resistance r_C of C_2. For instance, at $Q_1 = 5$ and $Q_o = 200$, $\eta_o = 97.5$ percent. To obtain high-efficiency η_o, Q_o should be as high as possible and Q_1 should be low. In contrast, the bandwidth of FM regulation of the dc output voltage V_o is narrower if Q_1 is higher. Therefore, the choice of Q_1 involves a reasonable trade-off.

Now the transfer function of the impedance inverter will be derived. As stated before, the power at the input of the impedance inverter L_3 for $Q_1 \geq 5$ contains the fundamental component only and is expressible as $P_{Ri} = V_1^2/R_i$, where V_1 is the rms value of the fundamental component v_1 given by (5). Neglecting power loss in L_3, $P_{Ri} = P_{oA}$. Thus, from (29) and (30), the ac-to-ac voltage transfer function of the impedance inverter is

$$M_I = \frac{V_i}{V_R} = \sqrt{\frac{R_i}{R}} = \sqrt{1 + q_B^2} = \sqrt{1 + \tan^2 \phi}. \quad (35)$$

It is apparent that $M_I \geq \sqrt{2}$ for $q_B \geq 1$.

Using (6), (33), and (35), one obtains the dc-to-dc voltage transfer function of the Class E converter of Fig. 1(a):

TABLE I
M_A AS A FUNCTION OF Q_1 AND D FOR OPTIMUM OPERATION

Q_1	D = 0.25	D = 0.50	D = 0.75
	M_A		
0	0.2025	0.5989	1.2777
1	0.2042	0.6331	1.2795
2	0.2078	0.6760	1.3409
3	0.2121	0.7011	1.3149
5	0.2193	0.7245	1.2876
7	0.2243	0.7349	1.2732
10	0.2289	0.7426	1.2617
20	0.2356	0.7513	1.2462
100	0.2407	0.7579	1.2321
∞	0.2439	0.7595	1.2280

$$M = \frac{V_o}{V_i} = \sqrt{\eta_A} M_A M_I M_R = \frac{\pi M_A \sqrt{\eta}\sqrt{1 + q_B^2}}{2\sqrt{2}n} \quad (36)$$

where η is the total converter efficiency and the values of M_A are given in Table I. For instance, for optimum operation at $D = 0.5$ and $Q_1 = 5$, $M = 0.8047 \cdot \sqrt{\eta}\sqrt{1 + q_B^2}/n$. Hence, $M = 1.138\sqrt{\eta}/n$ at $q_B = 1$.

V. Design Equations

The following converter specifications are usually supplied for the designer: V_i, V_o, and $P_{o\max}$. The converter can be designed so that the maximum output power $P_{o\max}$ occurs for optimum operation of the Class E inverter. In general, the operating point for $P_{o\max}$ should be located on the graph of Fig. 5(a) to the left of the maximum value (i.e., $q_B \geq 1$) to obtain lossless operation for $R_{L\min} \leq R_L \leq \infty$. The minimum value of the load resistance is

$$R_{L\min} = \frac{V_o^2}{P_{o\max}}. \quad (37)$$

Assuming n and substituting (37) into (20), we have

$$R_{i\min} = \frac{8n^2}{\pi^2} R_{L\min}. \quad (38)$$

Let us define the following parameters: $b = V_i^2 R/P_o$, $c = \omega C_1 R$, $d = \omega CR = \omega C_2 R$, and $e = \omega L/R$, where $C_2 = C$ and $L = L_2 + L_S$. The values of all of these parameters are given in [17] at any Q_1 and D for optimum operation of the Class E inverter. Assuming Q_1, D, and f, one can determine

$$R_{\max} = \frac{bV_i^2}{P_{o\max}}, \quad (39)$$

$$C_1 = \frac{c}{\omega R_{\max}}, \quad (40)$$

$$C_2 = \frac{d}{\omega R_{\max}}, \tag{41}$$

$$L = \frac{eR_{\max}}{\omega}. \tag{42}$$

From (30) and (39),

$$q_{B\min} = \sqrt{\frac{R_{i\min}}{R_{\max}} - 1}. \tag{43}$$

Using (31),

$$X_i = \frac{R_{i\min}}{q_{B\min}}, \tag{44}$$

which leads to

$$L_i = \frac{X_i}{\omega}. \tag{45}$$

From (31),

$$X_{LS\min} = \frac{X_i}{1 + \frac{1}{q_{B\min}^2}}, \tag{46}$$

which leads to

$$L_{S\min} = \frac{X_{LS\min}}{\omega}. \tag{47}$$

Hence, from (32),

$$L_2 = L - L_{S\min}. \tag{48}$$

From (22) and (44),

$$L_3 = \frac{\pi^2}{8} L_i. \tag{49}$$

Let us define $k = R_{L\max}/R_{L\min} = R_{i\max}/R_{i\min} = q_{B\max}/q_{B\min}$. Hence, from (30), one obtains $R_{\max}/R_{\min} = (1 + k^2 q_{B\min}^2)[k(1 + q_{B\min}^2)]$.

To obtain lossless operation at any value of R_L, one can assume $q_B = 1$ at $R_{i\min}$. In this case, the operating point for $P_{o\max}$ is located at the maximum value of the graph shown in Fig. 5(a). Equations (37)–(42) and (47)–(49) remain the same. From (43), (44), and (46),

$$X_i = R_{i\min} = 2R_{\max}, \tag{50}$$

$$X_{LS\min} = \frac{X_i}{2} = R_{\max}. \tag{51}$$

From (38) and (50),

$$n = \pi\sqrt{\frac{R_{i\min}}{8R_{L\min}}} = \frac{\pi}{2}\sqrt{\frac{R_{\max}}{2R_{L\min}}}. \tag{52}$$

Using (30) and (33), one obtains $R_{\max}/R_{\min} = (1 + k^2)/(2k)$. For example, at $k = 3$, $R_{\max}/R_{\min} = 1.67$; at $k = 5$, $R_{\max}/R_{\min} = 2.6$; and at $k = 10$, $R_{\max}/R_{\min} = 5$. Thus variations in R are much smaller than those in R_L.

Example: Design a dc/dc converter with the following specifications: $V_i = 28$ V, $V_o = 5$ V, $P_{o\max} = 10$ W, and $k = R_{L\max}/R_{L\min} = 3$.

Let us design the Class E dc/dc converter of Fig. 1(a) operating at the switching frequency $f = 2$ MHz for optimum operation. From (37), $R_{L\min} = V_o^2/P_{o\max} = 5^2/10 = 2.5\ \Omega$. $D2$ and $D3$ are assumed to be Schottky diodes with forward voltage drops $V_F = 0.5$ V. Hence, the rectifier efficiency $\eta_R = 1/(1 + V_F/V_o) = 1/(1 + 0.5/5) = 91$ percent. Assuming that the transformer efficiency is $\eta_t = 95$ percent and the Class E inverter efficiency is $\eta_A = 95$ percent, the total converter efficiency is $\eta = \eta_A\eta_t\eta_R = 0.95 \times 0.95 \times 0.91 = 0.82 = 82$ percent. Hence, the dc input power is $R_{i\max} = P_{o\max}/\eta = 10/0.82 = 12.2$ W and the dc input current is $I_{i\max} = P_{i\max}/V_i = 12.2/28 = 0.44$ A. The Class E inverter will be designed for optimum operation at $P_{o\max}$ with $D = 0.5$ and $Q_1 = 5$. From [17], $b = V_i^2 R/P_o = 0.5249$, $c = \omega C_1 R = 0.2067$, $d = \omega CR = \omega C_2 R = 0.2269$, and $e = \omega L/R = 5.673$. Hence, from (39)–(42), $R_{\max} = bV_i^2/P_{i\max} = 0.5249 \times 28^2/12.2 = 33.73\ \Omega$, $C_1 = c/(\omega R_{\max}) = 0.2067/(2 \times \pi \times 2 \times 10^6 \times 33.73) = 448$ pF, $C_2 = d/(\omega R_{\max}) = 0.2269/(2 \times \pi \times 2 \times 10^6 \times 33.73) = 535$ pF, and $L = eR_{\max}/\omega = 5.673 \times 33.73/(2 \times \pi \times 2 \times 10^6) = 15.23\ \mu$H. Assume that $q_B = 1$ at $R_{L\min}$. From (50) and (51), $X_i = R_{i\min} = 2R_{\max} = 2 \times 33.73 = 67.46\ \Omega$ and $X_{LS\min} = R_{\max} = 33.73\ \Omega$. Thus, $L_i = X_i/\omega = 67.46/(2 \times \pi \times 2 \times 10^6) = 5.37\ \mu$H and $L_{S\min} = L_i/2 = 2.68\ \mu$H. From (48), $L_2 = L - L_{S\min} = 15.23 - 2.68 = 12.55\ \mu$H. From (49), $L_3 = \pi^2 L_i/8 = \pi^2 \times 5.37/8 = 6.62\ \mu$H. From (50), $n = \pi\sqrt{R_{i\min}/(8R_{L\min})} = \pi\sqrt{64.46/(8 \times 2.5)} = 5.8$. From [17], $V_{SM} = 3.61\ V_i = 3.61 \times 28 = 101$ V and $I_{SM} = 2.783 I_{i\max} = 2.783 \times 0.44 = 1.225$ A. The maximum load current is $I_{o\max} = P_{o\max}/V_o = 10/5 = 2$ A. Hence, from (26) at $\phi = 45°$, the peak currents of the rectifier diodes are $I_{D2M} = I_{D3M} = 1.665 I_{o\max} = 1.665 \times 2 = 3.33$ A. From (28), $V_{D2MR} = V_{D3MR} = -2 \times 5 = -10$ V. The values of V_{SM}, I_{SM}, I_{D2M}, and I_{D3M} decrease with R_L as will be shown in Section VII. Therefore, their maximum values occur at $R_{L\min}$. The maximum value of the peak voltage across C_1 is equal to $V_{SM} = 101$ V. The peak voltage across L_3 is $nV_o = 5.8 \times 5 = 29$ V. Thus the peak-to-peak input voltage of the transformer is 58 V. Since $q_B = 1$ at $R_{L\min}$, (29) gives $\phi = 45°$. Hence, from (10), $I_m = \pi I_{o\max}/(2n \cos\phi) = \pi \times 2/(2 \times 5.8 \times \cos 45°) = 0.766$ A. The reactances of C_2 and L_2 are $X_{C2} = 1/\omega C_2 = 149\ \Omega$ and $X_{L2} = \omega L_2 = 158\ \Omega$ and therefore the peak value of the voltage across C_2 is $X_{C2} I_m = 149 \times 0.766 = 114$ V and the peak value of the voltage across L_2 is $X_{L2} I_m = 158 \times 0.766 = 121$ V. These two voltages can be reduced by choosing a smaller value of Q_1 at $R_{L\min}$. As R_L increases, the two voltages decrease because the value of I_m decreases with R_L. The maximum load resistance is $R_{L\max} = 3R_{L\min} = 3 \times 2.5 = 7.5\ \Omega$ and therefore $R_{i\max} = 3R_{i\min} = 3 \times 67.46 = 202.38\ \Omega$. From (29), $q_{B\max} = R_{i\max}/X_i = 3R_{i\min}/X_i = 3$, from which $\phi = 71.56°$. Since $k = 3$, $R_{\max}/R_{\min} = (1 + k^2)/(2k) = (1 + 3^2)/(2 \times 3) = 1.67$, which gives $R_{\min} = R_{\max}/1.67 = 33.73/1.67 = 20.2\ \Omega$.

VI. Family of Class E DC/DC Converters with an Inductive Impedance Inverter

Fig. 6 shows a family of the Class E resonant dc/dc converters with an impedance inverter. This family can be derived from the basic circuits of Class E dc/dc converters by adding the inductance L_3. In the converters of Fig. 6(a) and (b), a coupling capacitor C_f is also added between the inductor L_3 or the transformer secondary winding and the half-wave rectifiers for the following reason. Consider the converter of Fig. 6(a). For the continuous mode of operation, diodes $D2$ and $D3$ conduct alternately with a conduction duty cycle of 50 percent. Therefore, the input voltage of the rectifier is a square wave whose low level is zero and high level is V_o. Hence, the average value of the rectifier input voltage is $V_o/2$. On the other hand, the average value of the voltage across L_3 or the transformer secondary winding is zero. The coupling capacitor C_f removes this contradiction. The voltage across C_f is $V_o/2$. Consequently, the voltage v is a square wave with peak values $nV_o/2$ and $-nV_o/2$. Thus, the rectifier acts as a voltage doubler. For the converters of Fig. 6(a) and (b),

$$\tan\phi = \frac{n^2 R_L}{4X_{L3}}, \tag{53}$$

$$R_i = \frac{2n^2}{\pi^2} R_L \approx \frac{n^2 R_L}{5}, \tag{54}$$

$$M_R = \sqrt{\frac{R_L}{R_i}} = \frac{\pi}{n\sqrt{2}} \approx \frac{2.22}{n}. \tag{55}$$

For optimum operation at $D = 0.5$ and $Q_1 = 5$, $M = 1.609\sqrt{\eta}\sqrt{1 + q_B^2}/n$; at $q_B = 1$, $M = 2.276\sqrt{\eta}/n$. The continuous mode of operation occurs for $R_L < 2\pi X_{L3}/n^2$.

For the converter of Fig. 6(c),

$$\tan\phi = \frac{n^2 R_L}{2X_{L3}}, \tag{56}$$

$$R_i = \frac{4n^2}{\pi^2} R_L \approx \frac{n^2 R_L}{2.5}, \tag{57}$$

$$M_R = \sqrt{\frac{R_L}{R_i}} = \frac{\pi}{2n} \approx \frac{1.57}{n}. \tag{58}$$

For optimum operation at $D = 0.5$ and $Q_1 = 5$, $M = 1.138\sqrt{\eta}\sqrt{1 + q_B^2}/n$; at $q_B = 1$, $M = 1.609\sqrt{\eta}/n$. The continuous mode of operation occurs for $R_L < \pi X_{L3}/n^2$. In addition, I_{DM}/I_o of the converters in Fig. 6(a)–(c) is twice that of the converter in Fig. 1(a). For the converter of Fig. 6(e), R_i is given by (17). All design equations given in Section V are the same for all converters of Fig. 6. The only difference is that (38) should be replaced by (53) for the converters of Fig. 6(a) and (b), and by (54) for the converter of Fig. 6(c).

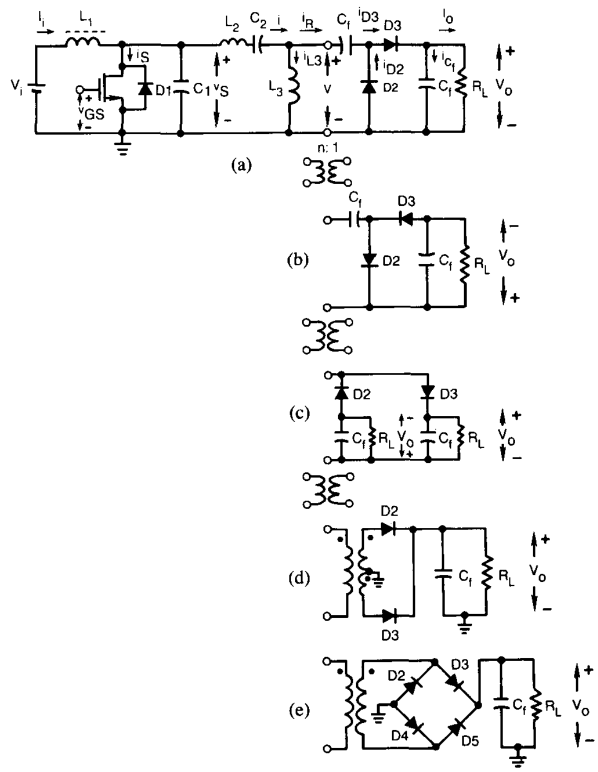

Fig. 6. Family of Class E resonant dc/dc converters with an inductive impedance inverter.

VII. Experimental Results

To demonstrate the feasibility of the Class E dc/dc converter with an inductive impedance inverter, the transformerless converter of Fig. 6(a) was designed and built, using an IRF620 MOSFET, IR31DQ06 diodes, $L_1 = 100$ μH, $C_1 = 1.35$ nF, $C_2 = 1.8$ nF, $L_2 = 15$ μH, $L_3 = 7.85$ μH, $C_f = 66$ nF, $V_i = 28$ V, and for optimum operation $D = 0.5$, $Q_1 = 5$, $f = 1$ MHz, and $R_{L\min} = 200$ Ω. The measured converter parameters for optimum operation were: $V_o = 55$ V, $P_o = 15.1$ W, $\eta = 89.3$ percent, and $M = 55/28 = 1.964$. Using the measured efficiency η, the theoretical value of the dc-to-dc voltage transfer function was $M = 2.276\sqrt{0.893} = 2.15$. Thus, the error was 9.47 percent. Next, the load resistance R_L was gradually increased from $R_L = 200$ Ω to infinity and the switching frequency f was also increased so that the dc output voltage V_o was held constant at 55 V. The switching frequency f at an open circuit at the output was 1.12 MHz. The relative bandwidth required to maintain V_o at 55 V over a wide range of R_L (from 200 Ω to infinity) was only 12 percent. Thus, the circuit is a narrow-band FM converter. Fig. 7 shows the current and voltage waveforms at $R_{L\min} = 200$ Ω (optimum operation), $R_L = 300$ Ω (the continuous mode of operation), and $R_L = 3$ kΩ (the discontinuous mode of operation). As seen, the experimental waveforms were close to those predicted theoretically. The peak values of all the currents and voltages decreased with R_L; the only exception was the peak-to-peak value of

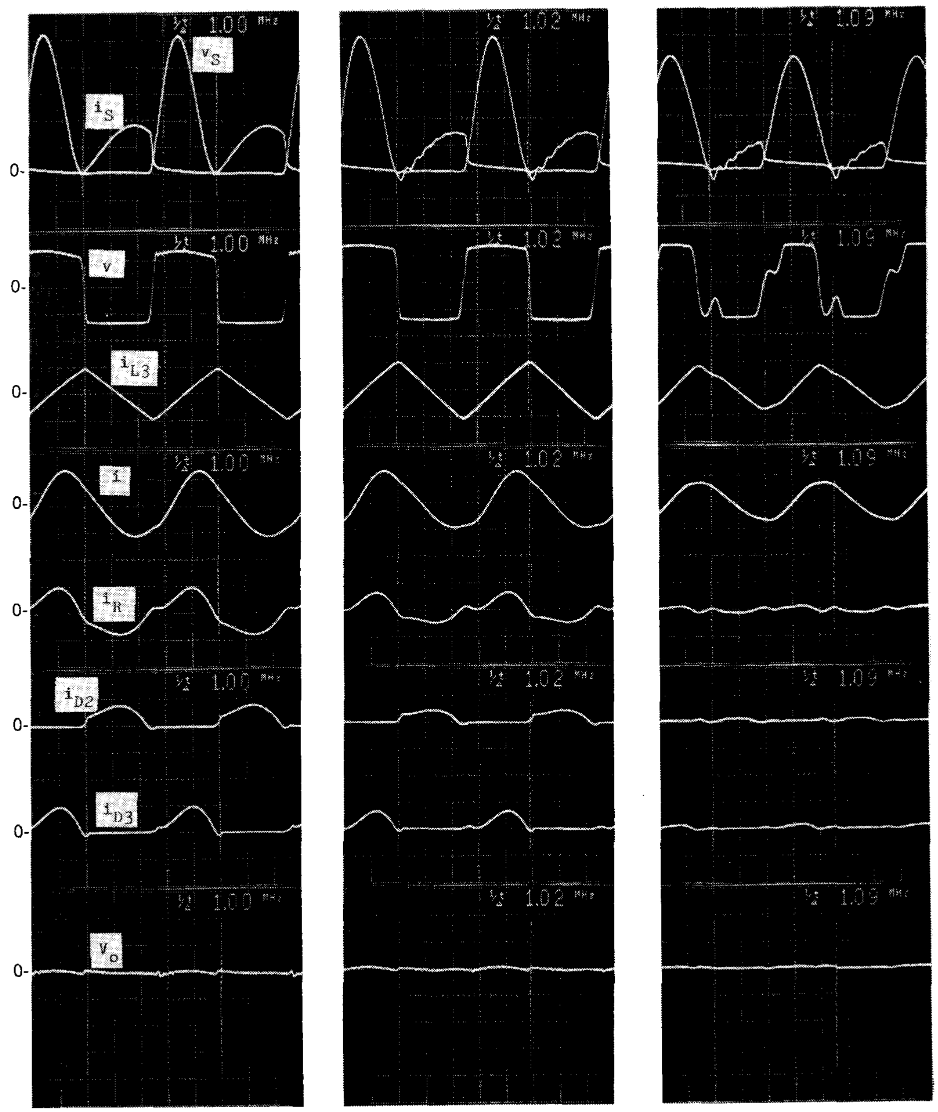

Fig. 7. Experimental current and voltage waveforms in converter of Fig. 6(a). (a) For optimum operation (R_L = 200 Ω). (b) For continuous mode of operation (R_L = 300 Ω). (c) For discontinuous mode of operation (R_L = 3 kΩ). Vertical: 1 A/div. for all currents, 20 V/div. for v_S and v, and 1 V/div. for ac component of V_o; horizontal: 200 ns/div.

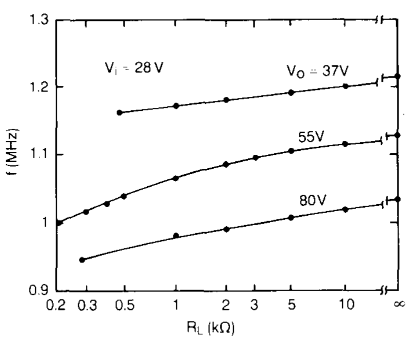

Fig. 8. Switching frequency f as a function of the load resistance R_L at constant values of dc output voltage V_o.

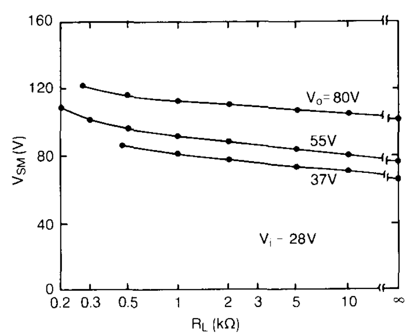

Fig. 9. Peak values of switch voltage V_{SM} as a function of R_L at constant values of V_o.

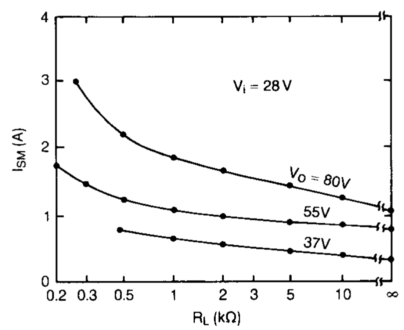

Fig. 10. Peak values of switch current I_{SM} as a function of R_L at constant values of V_o.

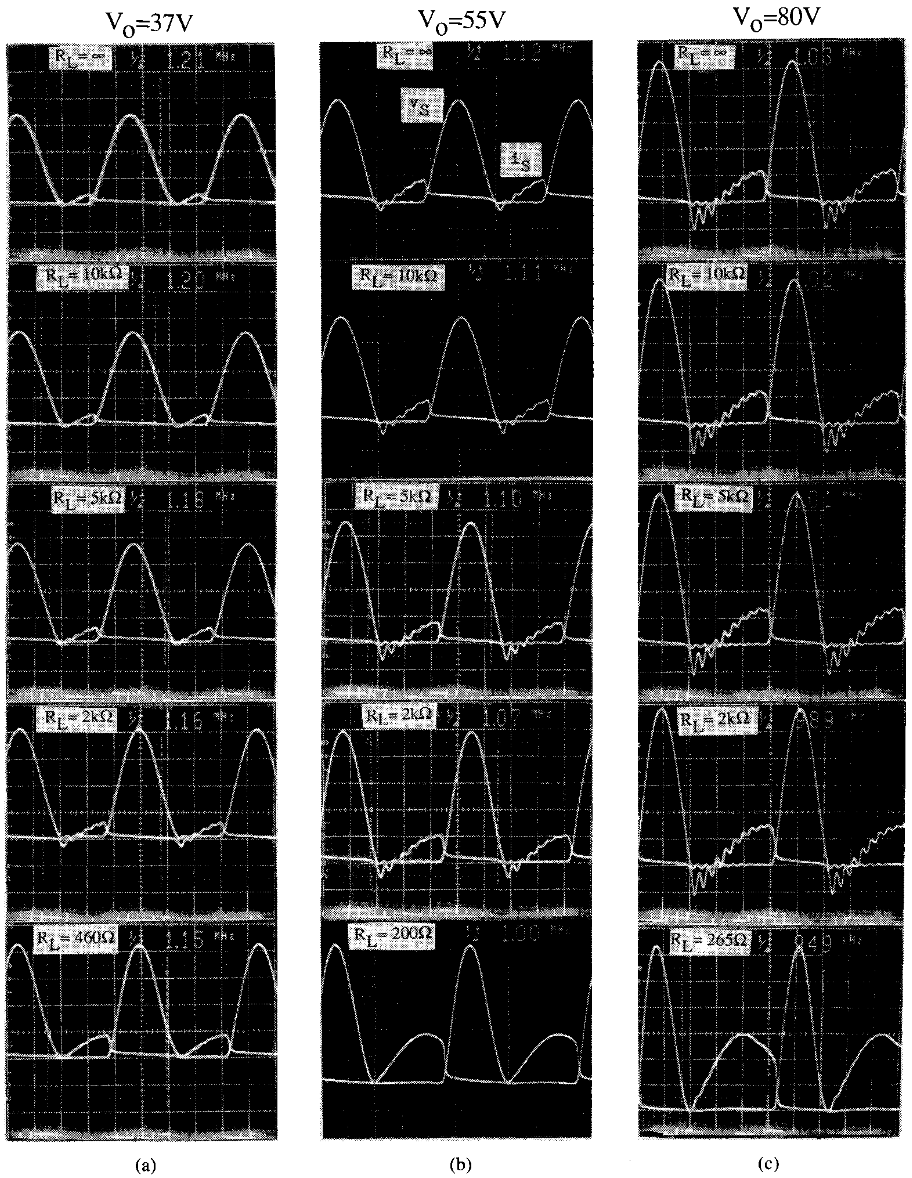

Fig. 11. Waveforms of drain current i_S and drain-to-source voltage v_S at various values of R_L. (a) For V_o = 37 V. (b) For V_o = 55 V. (c) For V_o = 80 V. Vertical: 1 A and 20 V/div.; horizontal: 200 ns/div.

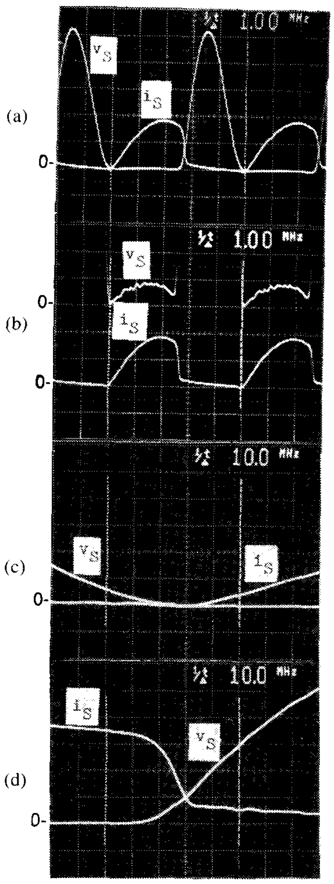

Fig. 12. Waveforms of i_S and v_S illustrating power losses in MOSFET for optimum operation at $D = 0.5, f = 1$ MHz, $R_{L\min} = 200\ \Omega$, and $V_o = 55$ V. (a) i_S and v_S (1 A, 20 V, and 200 ns/div.). (b) v_S and i_S illustrating conduction loss (1 V, 1 A, and 200 ns/div.). (c) v_S and i_S at turn-on (20 V, 0.5 A, and 20 ns/div.). (d) i_S and v_S at turn-off (0.5 A, 20 V, and 20 ns/div.).

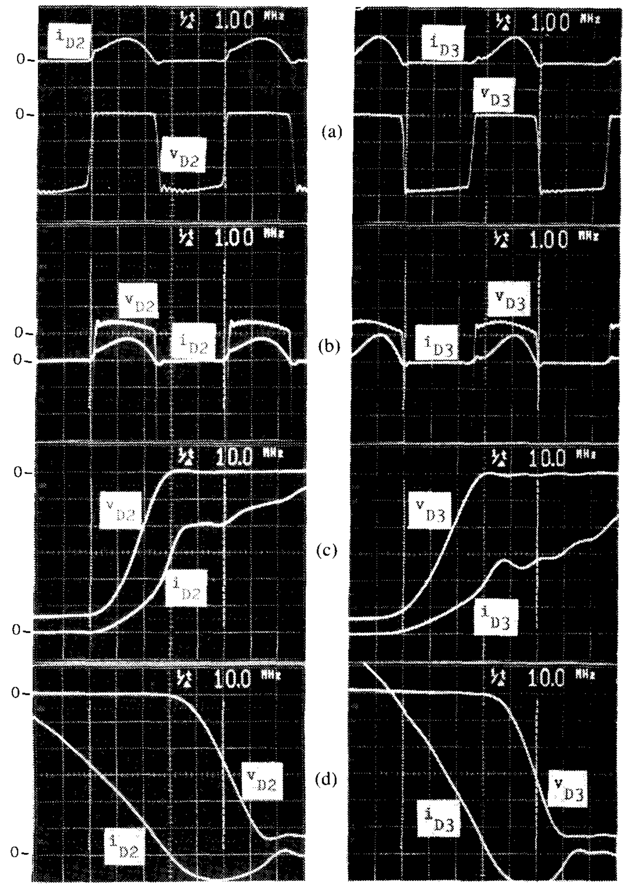

Fig. 13. Waveforms of rectifier diodes at $f = 1$ MHz, $R_{L\min} = 200\ \Omega$, and $V_o = 55$ V. (a) i_{D2}, v_{D2}, i_{D3}, v_{D3} (1 A, 20 V, and 200 ns/div.). (b) Waveforms illustrating conduction losses (1 V, 1 A, and 200 ns/div.). (c) Waveforms illustrating turn-on switching losses (10 V, 0.1 A, and 20 ns/div.). (d) Waveforms illustrating turn-off losses (10 V, 0.1 A, and 20 ns/div.).

v which was constant. For optimum operation and the continuous mode of operation, the waveforms were approximately free of parasitic oscillations. For the discontinuous mode of operation, voltage v differs from a square wave and current i_L differs from a triangle wave. Nevertheless, it was easy to maintain V_o at 55 V. The maximum value of the peak-to-peak ripple voltage was $V_{r\max} = 0.2$ V; hence $V_{r\max}/V_o = 0.36$ percent. The output voltage was very smooth, without spikes and noise.

Fig. 8 depicts the switching frequency f as a function of the load resistance R_L at constant values of V_o. The characteristic at $V_o = 55$ V corresponds to $D = 0.5, f = 1$ MHz, and $R_{L\min} = 200\ \Omega$ for optimum operation, as previously described. The characteristic at $V_o = 37$ V corresponds to $D = 0.44, f = 1.15$ MHz, and $R_{L\min} = 460\ \Omega$ for optimum operation. The characteristic at $V_o = 80$ V corresponds to $D = 0.61, f = 0.949$ MHz, and $R_{L\min} = 265\ \Omega$ for optimum operation (in this case, $D2$ and $D3$ were composed of two diodes connected in series). All other components were the same as at $V_o = 55$ V. It can be seen that different values V_o can be obtained by varying the value of D and f for optimum operation. The values of the dc voltage transfer function $M = V_o/V_i$ were 1.32, 1.96, and 2.86 at $V_o = 37$, 55, and 80 V, respectively. Figs. 9 and 10 show the peak values of the switch voltage V_{SM} and the switch current I_{SM} versus R_L at constant values of V_o. As shown, both V_{SM} and I_{SM} decreased with R_L. Fig. 11 shows the waveforms of i_S and v_S at various values of R_L for $V_o = 37$, 55, and 80 V. As seen, the lossless operation (i.e., zero-voltage-switching) was obtained in all three cases for the entire range of R_L, from full-load resistance $R_{L\min}$ to infinity ($R_L = \infty$). The switching frequency f was varied from 1.15 to 1.21 MHz at $V_o = 37$ V and from 0.949 to 1.03 MHz at $V_o = 80$ V. Thus, the values of $\Delta f/f_{\text{opt}}$ were 5.2 and 8.5 percent, respectively. The peak values of the voltages across L_2 and C_2 decreased with R_L. For instance, at $V_o = 55$ V, the peak value of the voltage across L_2 decreased from 129 to 71 V and the peak value of the voltage across C_2 decreased from 102 to 56 V as R_L was increased from 200 Ω to infinity. The highest peak values of all currents and voltages occur at $R_{L\min}$.

Fig. 12 shows the waveforms of i_S and v_S in the enlarged scales to illustrate power losses in the MOSFET. The waveforms in Fig. 12(b) illustrate the conduction loss. The peak value of v_S was 1 V when the transistor was ON. Hence, the transistor on-resistance was $r_{DS} = 1\ \mathrm{V}/2\ \mathrm{A} = 0.5\ \Omega$. The dc input current was 0.604 A. Thus, the conduction loss was $P_{CDS} = 2.37 r_{DS} I_i^2 = 0.432$ W. The waveforms of v_S and i_S at turn-on are shown in Fig. 12(c). The turn-on switching loss was zero because i_S and v_S were *not* overlapping at turn-on. Fig. 12(d) shows the waveforms of i_S and v_S at turn-off. When the voltage v_S begins to increase, the current i_S decreases from $2I_i$ to zero. The transition time interval was 20 ns, which was 2 percent of the period $T = 1/f = 1000$ ns. The turn-off switching loss was nonzero because i_S and v_S were overlapping during turn-off [11].

Fig. 13 shows the waveforms of the rectifier diodes in the enlarged scales to illustrate power losses in these diodes. Fig. 13(b) illustrates the conduction losses. The forward diode voltages were approximately $V_F = 0.5$ V. The dc output current was $I_o = 0.275$ A. Hence, the conduction loss in each diode was $P_{CDR} = V_F I_o / 2 = 69$ mW. The waveforms during turn-on are shown in Fig. 13(c). As v_{D2} and v_{D3} increase from -55 to 0.5 V, i_{D2} increases from zero to 0.3 A and i_{D3} increases from zero to 0.2 A. The transition time intervals were 50 ns for both diodes. Fig. 13(d) shows the waveforms during turn-off. The diode voltages begin to decrease from 0.5 to -55 V as the diode currents reach zero. Next, the diode currents are negative during the reverse-recovery time.

VIII. Conclusion

The analysis, design procedure, and experimental results have been presented for the Class E resonant dc/dc converters with an inductive impedance inverter. It is shown that lossless converter operation can be obtained over a wide range of the load resistance, from zero to infinity. However, the practical range of R_L is from $R_{L\min} = V_o^2/P_{o\max}$ to infinity. The bandwidth of the switching frequency f required to regulate the dc output voltage V_o is very narrow. The measured values of $\Delta f / f_{\mathrm{opt}}$ for $R_{L\min} \leq R_L \leq \infty$ were 5.2, 12, and 8.5 percent at $V_o = 37$, 55, and 80 V, respectively. Therefore, the Class E converters are narrow-band frequency-modulated (NBFM) converters. The same rules can also be applied in other resonant converters, e.g., in converters derived from Class D tuned power amplifiers. The Class E dc/dc converters may be improved by using resonant rectifiers proposed in [30], [33].

References

[1] N. O. Sokal and A. D. Sokal, "Class E—A new class of high-efficiency tuned single-ended switching power amplifiers," *IEEE J. Solid-State Circuits*, vol. SC-10, pp. 168–176, June 1975.

[2] ——, "Class E switching-mode RF power amplifiers—Low power dissipation, low sensitivity to component tolerance (including transistors), and well-defined operation," presented at the IEEE ELECTRO '79 Conf., Session 23, New York, NY, Apr. 25, 1979. Reprinted in *R. F. Design*, vol. 3, no. 7, pp. 33–38, 41, July/Aug. 1980.

[3] F. H. Raab, "Idealized operation of the Class E tuned power amplifier," *IEEE Trans. Circuits Syst.*, vol. CAS-24, pp. 725–735, Dec. 1977.

[4] ——, "Effects of circuit variations in the Class E tuned power amplifier," *IEEE J. Solid-State Circuits*, vol. SC-13, pp. 239–247, Apr. 1978.

[5] F. H. Raab and N. O. Sokal, "Transistor power losses in the Class E tuned power amplifiers," *IEEE J. Solid-State Circuits*, vol. SC-13, pp. 912-914, Dec. 1978.

[6] J. Ebert and M. Kazimierczuk, "High efficiency RF power transistor amplifier," *Bull. Acad. Pol. Sci., Ser. Sci. Tech.*, vol. 25, no. 2, pp. 135–138, 1977.

[7] ——, "Class E high-efficiency tuned power oscillator," *IEEE J. Solid-State Circuits*, vol. SC-16, pp. 62-66, Apr. 1981.

[8] M. Kazimierczuk, "High-efficiency tuned transistor power amplifier" (in Polish), Ph.D. dissertation, Tech. Univ. Warsaw, Poland, 1977.

[9] ——, "Theory of the Class E tuned power amplifier" (in Polish), *Rozpr. Elektrot.*, vol. 25, no. 4, pp. 957-986, 1979.

[10] ——, "Theoretical analysis of the Class E tuned power amplifier at any switch duty ratio" (in Polish), *Rozpr. Elektrot.*, vol. 25, no. 4, pp. 987-1003, 1979.

[11] ——, "Effects of the collector current fall time on the Class E tuned power amplifier," *IEEE J. Solid-State Circuits*, vol. SC-18, pp. 181–193, Apr. 1983.

[12] ——, "Parallel operation of power transistors in switching amplifiers," *Proc. IEEE*, vol. 71, pp. 1456–1457, Dec. 1983.

[13] ——, "High efficiency tuned power amplifiers, frequency multipliers, and oscillators" (in Polish), Dr. Hab. dissertation, Tech. Univ. Warsaw, Poland, 1984.

[14] B. Molnár, "Basic limitations of waveforms achievable in single-ended switching-mode (Class E) power amplifiers," *IEEE J. Solid-State Circuits*, vol. SC-19, pp. 144–146, Feb. 1984.

[15] M. K. Kazimierczuk, "Generalization of conditions for 100-percent efficiency and nonzero output power in power amplifiers and frequency multipliers," *IEEE Trans. Circuits Syst.*, vol. CAS-33, pp. 805-807, Aug. 1986.

[16] ——, "Class E tuned power amplifier with nonsinusoidal output voltage," *IEEE J. Solid-State Circuits*, vol. SC-21, pp. 575–581, Aug. 1986.

[17] M. K. Kazimierczuk and K. Puczko, "Exact analysis of Class E tuned amplifier at any Q and switch duty cycle," *IEEE Trans. Circuits Syst.*, vol. CAS-34, pp. 149–159, Feb. 1987.

[18] ——, "Class E tuned power amplifier with antiparallel diode or series diode at switch with any Q and switch duty cycle," *IEEE Trans. Circuits Syst.*, submitted.

[19] R. E. Zulinski and J. W. Steadman, "Class E power amplifiers and frequency multipliers with finite dc-feed inductance," *IEEE Trans. Circuits Syst.*, vol. CAS-34, pp. 1074–1087, Sept. 1987.

[20] M. K. Kazimierczuk, "High-speed driver for switching power MOSFETs," *IEEE Trans. Circuits Syst.*, vol. 35, pp. 254–256, Feb. 1988.

[21] R. J. Gutmann, "Application of RF circuit design principles to distributed power converters," *IEEE Trans. Ind. Electron. Contr. Instrum.*, vol. IECI-27, pp. 156-164, Aug. 1980.

[22] R. Redl, B. Molnár, and N. O. Sokal, "Class E resonant regulated dc/dc power converters: Analysis of operation and experimental results at 1.5 MHz," *IEEE Trans. Power Electron.*, vol. PE-1, pp. 111-120, Apr. 1986.

[23] ——, "Small-signal dynamic analysis of regulated Class-E dc/dc converters," *IEEE Trans. Power Electron.*, vol. PE-1, pp. 121–128, Apr. 1986.

[24] R. Redl and B. Molnár, "Design of a 1.5-MHz regulated dc/dc power converter," in *Proc. 7th Int. PCI Conf. on Power Conversion* (Geneva, Switzerland), pp. 74-87, Sept. 1983.

[25] R. Redl and N. O. Sokal, "High-frequency switching-mode power converters: General considerations and design examples at 0.6, 1, and 14 MHz" (tutorial), in *Proc. First Int. High Frequency Power Conversion Conf.*, Virginia Beach, VA, May 28-30, 1986.

[26] ——, "A 14-MHz 100-Watt Class E resonant converter: Principles, design considerations, and measured performance," in *Proc. Power Electronics Conf.*, San Jose, CA, Oct. 7, 1986.

[27] M. K. Kazimierczuk and K. Puczko, "Impedance inverter for Class E dc/dc converter," in *Proc. 29th Midwest Symp. on Circuits and Systems*, Lincoln, NE, Aug. 11-12, 1986, pp. 707-710.

[28] N. O. Sokal, R. Redl, and B. Molnár, "Class E high-frequency high-efficiency dc/dc power converter," U.S. Patent No. 4,607,323, Aug. 19, 1986.

[29] M. K. Kazimierczuk and K. Puczko, "Control circuit for Class E resonant dc/dc converter," in *Proc. IEEE Nat. Aerospace and Electronics Conf. (NAECON '87)*, Dayton, OH, May 18–22, 1987, pp. 416–423.

[30] W. C. Bowman, F. M. Magalhaes, W. B. Suiter, and N. G. Ziesse, "Resonant rectifier circuit," U.S. Patent No. 4,685,041, Aug. 4, 1987.

[31] M. K. Kazimierczuk and X. T. Bui, "A family of Class E resonant dc/dc power converters," in *Proc. 16th Int. Power Electronics (PCI '88) Conf. (SATECH '88)*, Dearborn, MI, Oct. 3–6, 1988, pp. 69–93.

[32] ——, "Class E dc/dc converters with a capacitive impedance inverter," *IEEE Trans. Industrial Electronics*, submitted.

[33] M. K. Kazimierczuk and J. Jóźwik, "Class E resonant rectifiers," in *Proc. 31st Midwest Symp. on Circuits and Systems* (St. Louis, MO), Aug. 10–12, 1988.

Marian K. Kazimierczuk was born in Poland on March 3, 1948. He received the M.S., Ph.D., and Habilitate Doctorate degrees in electronics engineering from the Department of Electronics, Technical University of Warsaw, Warsaw, Poland, in 1971, 1978, and 1984, respectively.

In 1972, he joined the Institute of Radio Electronics, Department of Electronics, Technical University of Warsaw, where he was employed as an Instructor from 1972 to 1978 and as an Assistant Professor from 1978 to 1984. He headed the Radio Electronics Laboratory and the Electronic Apparatus Laboratory from 1978 to 1984. His teaching, research, and development activities were in the areas of RF power technology, radio transmitters, electronic circuits and systems, semiconductor device modeling, electromagnetic field theory, microwave theory and technique, electronic measurements, circuit theory, communications, and computer-aided design. In 1984, he worked as a Project Engineer at Design Automation, Inc., Lexington, MA, where he was responsible for designing Class E high-efficiency switching-mode dc/dc converters. In 1984–1985, he was a Visiting Professor with the Department of Electrical Engineering, Virginia Polytechnic Institute and State University, Blacksburg, VA, where he taught electromagnetic fields and electronic circuits and systems, and his research activity was in the area of power electronics. Since 1985 he has been an Assistant Professor with the Department of Electrical Systems Engineering, Wright State University, Dayton, OH, where he has been working in the areas of analog and digital electronics, integrated circuits, electronic devices, and power electronics. He is the author of 60 scientific papers, of which 19 were published in IEEE Transactions and Journals. He also holds six patents related to the new concepts of high-efficiency switching-mode tuned power amplifiers and oscillators.

Dr. Kazimierczuk is a member of the Association of Polish Engineers and the Polish Society of Theoretical and Applied Electrical Sciences. He received seven awards from the President of the Technical University of Warsaw, three awards from the Polish Ministry of Science, University Education, and Technology in 1981, 1982, and 1985, and an award from the Polish Academy of Sciences in 1983 for scientific achievements.

Xung T. Bui was born in Vietnam on February 20, 1947. He received the B.S. degree in electrical engineering from Wright State University, Dayton, OH, in 1987, and is now a graduate student there working towards the M.S. degree in electrical engineering.

He worked as a Teaching Assistant at Wright State University for two years. Currently he is an Associate Systems Engineer at SofTech Inc., Dayton, OH. His research interests are in the areas of tuned power transistor amplifiers, resonant dc/dc power converters, communication systems, and computer-aided design.